

**Empirical evaluation of three-electron quantum-electrodynamics effects  
from lithiumlike resonance lines of elements  $Z = 22-42$   
in the Tokamak Fusion Test Reactor and Joint European Torus tokamaks**

E. Hinnov and the TFTR Operating Team

*Plasma Physics Laboratory, Princeton University, Princeton, New Jersey 08543*

B. Denne and the JET Operating Team

*JET Joint Undertaking, Abingdon, Oxon, OX14 3EA, United Kingdom*

(Received 20 April 1989)

Most of the lithiumlike-ion resonance-line wavelengths have been remeasured relative to well-established lines of He II and C V, C VI in the Tokamak Fusion Test Reactor and to these are added the newly measured lines of Kr XXXIV and Mo XL from the Joint European Torus, which allow a systematic evaluation of differences from calculated one-electron Lamb shifts.

## I. INTRODUCTION

The lithium-sequence resonance lines, corresponding to the transitions  $2s_{1/2}-2p_{1/2}$  and  $2s_{1/2}-2p_{3/2}$ , possess some unique advantages for the purpose of diagnosing tokamak-type plasmas. They are quite strong and relatively isolated from other lines of neighboring ionization stages of the same element. Their excitation potential, especially for heavier elements, is small compared to the ionization potential. As it is the ionization potential that principally determines the radial location of the ion, this means that the local electron temperature is large compared to the excitation potential and hence the brightness of the lines is practically independent of the electron temperature in a given discharge, provided that it is high enough to produce the lithiumlike state. The latter condition implies that the central electron temperature,  $T_e(0)$  satisfies

$$T_e(0) \approx E_i \gg E_x, \quad (1)$$

with  $E_i$  and  $E_x$  the ionization potential of the lithiumlike state and the excitation potential of the line, respectively.

Also, as it is usually the central or highest-temperature ions that are of primary interest, Eq. (1) determines the element that is appropriate in a given tokamak discharge. Thus in the ST (Symmetric Torus) tokamak, with  $T_e(0) \sim 2$  keV, it was iron and chromium; in the PLT (Princeton Large Torus) tokamak, with  $T_e(0) \sim 2-3$  keV, it was nickel and copper; whereas the TFTR (Tokamak Fusion Test Reactor) has produced germanium and selenium in lithiumlike states, and the JET (Joint European Torus) tokamak, with its large size and powerful rf heating, has been recently capable of raising molybdenum to the lithiumlike state.<sup>1</sup>

While for plasma diagnostics, which depend on line intensity or Doppler-shift measurements, the absolute accuracy of the wavelengths is not very important (about  $\pm 0.1-0.3$  Å is generally all that is required), these lithium-sequence lines are also of vital interest to atomic physics; precision measurements of the transition wave-

lengths can be used to test QED and relativistic corrections. The importance of such measurements for many-electron systems was pointed out long ago by Berry, DeSerio, and Livingston,<sup>2</sup> and again emphasized in a recent article by Johnson, Blundell, and Sapirstein.<sup>3</sup> For such studies, measurement accuracy is at a premium. It is for this reason that we have made an effort to present our results with the maximum feasible precision, including also a reevaluation of our previous results with respect to better reference lines. We hope the present results will be of use for critical comparisons with theoretically calculated values.

## II. EXPERIMENTAL RESULTS

The wavelengths of the lines up to selenium were measured in Ohmically heated discharges of TFTR into which the appropriate element was injected by means of laser ablation. The krypton wavelengths were measured on the JET tokamak<sup>4</sup> into which krypton was admitted by means of a fast valve. The molybdenum was measured in JET plasmas heated by both Ohmic current and rf, by which means around 10 keV electron temperature could be reached.

It is generally not difficult to identify the lithiumlike doublet, especially in the step-by-step fashion in which the experiments were performed. The wavelengths were measured by Schwob-Fraenkel spectrometers, which admit about 40 Å sections of spectrum at a time, scanning this section repeatedly throughout the discharge. As wavelength standards we tried to use wherever possible the various orders of the resonance lines of C VI and C V, which are copiously emitted by these discharges, and are generally observable to the ninth and eighth grating orders, respectively.

For the wavelengths of the C V resonance and intercombination lines, Edlén and Löfstrand<sup>5</sup> have given 40.2680–40.7306 Å, or the difference of 0.4626 Å. Although our measurements do not approach such accura-

cy, comparison of higher orders indicates consistently a wavelength difference  $\sim 0.0003 \text{ \AA}$  smaller—except in the fifth order, where the intercombination line appears to be blended by something else. Accordingly, we have taken the resonance wavelength to be  $40.2683 \text{ \AA}$ , as may be consistent with the discussion by Edlén and Löfstrand. Likewise, the second singlet line, observable in our spectra to third order, we have taken as  $34.9728 \text{ \AA}$ . The iron, nickel, and titanium lines were remeasured in helium discharges, using He II lines as references. The He II and C VI wavelengths we use are those of Garcia and Mack.<sup>6</sup>

The results of our measurements are given in Table I together with the estimated error limits. In almost all cases the line from  $p_{1/2}$  was measurable with more precision in spite of its lower intensity and the fact that they were only measured in the first order, since the spectrometer wavelength coverage extends only to about  $330 \text{ \AA}$ . This is because the quoted wavelengths depend rather critically on one or two reference wavelengths. Thus in Ti XX the  $s_{1/2}-p_{1/2}$  line is between the He II resonance line at  $303.783 \text{ \AA}$  and a C IV line at  $312.432 \text{ \AA}$  while the  $s_{1/2}-p_{3/2}$  depends mostly on C V in the sixth order— $241.610 \text{ \AA}$ , and the C VI line in the eighth order— $269.888 \text{ \AA}$ . Also the  $s_{1/2}-p_{1/2}$  lines in Fe XXIV and Ni XXVI are accurately measured with respect to He II lines at  $256.317 \text{ \AA}$  and  $234.347 \text{ \AA}$ , respectively, while the  $s_{1/2}-p_{3/2}$  line of Fe XXIV was measured only relative to the O V triplet at  $192.85 \text{ \AA}$ . The Ni XXVI  $s_{1/2}-p_{3/2}$  line is more fortunate; it is in the proximity of C VI in the fifth order at  $168.680 \text{ \AA}$ . From Cu XXVII on, the  $s_{1/2}-p_{3/2}$  lines could be measured in second order and the Kr XXXIV in third order (while

TABLE I. Measured wavelengths of the lithium sequence resonance lines in  $\text{\AA}$ .

Ion	$\lambda(s_{1/2}-p_{1/2})$	$\lambda(s_{1/2}-p_{3/2})$	Source
Ti XX	$309.065 \pm 0.015$	$259.300 \pm 0.02$	TFTR
Cr XXII	$279.729 \pm 0.02$	$223.010 \pm 0.02$	TFTR
Fe XXIV	$255.094 \pm 0.01$	$192.012 \pm 0.02$	TFTR
Ni XXVI	$234.155 \pm 0.01$	$165.396 \pm 0.01$	TFTR
Cu XXVII	$224.795 \pm 0.01$	$153.507 \pm 0.02$	TFTR
Ge XXX	$200.290 \pm 0.01$	$122.705 \pm 0.02$	TFTR
Se XXXII	$186.375 \pm 0.015$	$105.686 \pm 0.02$	TFTR
Kr XXXIV	$174.036 \pm 0.026$	$91.049 \pm 0.025$	JET
Mo XL	$143.998 \pm 0.02$	$58.499 \pm 0.02$	JET

the second order was blended by the strong C VI  $n=2-3$  complex at  $\sim 182.11 \text{ \AA}$ ). Also the Mo lines could in principle be measured very accurately in higher orders but for the restrictions on machine time.

### III. COMPARISON WITH CALCULATIONS

In Table II are given the wave numbers for the  $s_{1/2}-p_{1/2}$  transition. The column marked  $\sigma_c$  shows the calculated values by Johnson, Blundell, and Sapirstein,<sup>3</sup> which do not include the QED effects, and a number of these we have interpolated from their Table III. The column with  $\sigma_x$  shows the experimental wave numbers together with the uncertainties as given in Table I, and  $\Delta(c-x)$  is their difference that is presumably ascribable to the QED

TABLE II. Calculated (Ref. 3) ( $c$ ) and experimental ( $x$ ) wave numbers ( $\text{cm}^{-1}$ ) and their differences compared to the one-electron QED effects, and the apparent screening by the 1s electrons, for the  $2s_{1/2}-2p_{1/2}$  transition. Numbers in parentheses denote interpolated values.

Z	$\sigma_c$	$\sigma_x$	$\Delta(c-x)$	1-el QED <sup>a</sup>	$-\delta\sigma_{1/2}$ (screening correction)
22	325 707	$323\,557 \pm 15$	$2150 \pm 15$	2532	$382 \pm 15$
24	360 463	$357\,489 \pm 25$	$2974 \pm 25$	3413	$439 \pm 25$
26	395 945	$392\,012 \pm 15$	$3933 \pm 15$	4490	$557 \pm 15$
27	(413 983) <sup>b</sup>	$\langle 409\,456 \rangle^c$	(4527)	5110	(583)
28	432 233	$427\,068 \pm 18$	$5165 \pm 18$	5784	$619 \pm 18$
29	(450 704) <sup>b</sup>	$444\,850 \pm 20$	$5854 \pm 20$	6522	$668 \pm 20$
30	469 406	$\langle 462\,819 \rangle^c$	(6587)	7320	(733)
32	(507 548) <sup>b</sup>	$499\,276 \pm 25$	$8272 \pm 25$	9116	$844 \pm 25$
34	(546 738) <sup>b</sup>	$536\,552 \pm 45$	$10\,185 \pm 45$	11 204	$1018 \pm 45$
36	587 062	$574\,594 \pm 85$	$12\,468 \pm 85$	13 598	$1130 \pm 85$
38	(628 612) <sup>b</sup>	$\langle 613\,562 \rangle^c$	(15 070)	16 349	(1279)
40	(671 486) <sup>b</sup>	$\langle 653\,479 \rangle^c$	(18 007)	19 456	(1449)
41	693 452	$\langle 673\,741 \rangle^c$	(19 711)	21 250	(1539)
42	(715 788) <sup>b</sup>	$694\,454 \pm 96$	$21\,334 \pm 96$	22 956	$1622 \pm 96$
44	(761 626) <sup>b</sup>	$\langle 736\,574 \rangle^c$	(25 052)	26 880	(1828)
45	(785 154) <sup>b</sup>	$\langle 758\,063 \rangle^c$	(27 091)	29 023	(1932)
47	(833 493) <sup>b</sup>	$\langle 802\,018 \rangle^c$	(31 475)	33 623	(2148)
50	(909 384) <sup>b</sup>	$\langle 870\,395 \rangle^c$	(38 989)	41 487	(2498)

<sup>a</sup>Reference 7, Table II less finite nuclear size effects.

<sup>b</sup>Our interpolations from Table III, Ref. 3.

<sup>c</sup>Interpolation from experimental data.

TABLE III. As Table II for the  $2s_{1/2}-2p_{3/2}$  transition. Numbers in parentheses denote interpolated values.

$Z$	$\sigma_c$	$\sigma_x$	$\Delta(c-x)$	1-el QED <sup>a</sup>	$-\delta\sigma_{3/2}$ (screening correction)
22	387 706	385 654±30	2052±30	2346	294±30
24	451 170	448 410±40	2760±40	3152	392±40
26	524 423	520 800±55	3623±55	4133	510±55
27	(565 299) <sup>b</sup>	(561 135) <sup>c</sup>	(4164)	4695	(531)
28	609 338	604 610±36	4728±36	5308	580±36
29	(656 801) <sup>b</sup>	651 436±85	5365±85	5975	610±85
30	707 964	(701 300) <sup>c</sup>	(6664)	7320	(656)
32	(822 559) <sup>b</sup>	814 963±130	7596±130	8320	724±130
34	(955 575) <sup>b</sup>	946 199±180	9376±180	10 199	823±180
36	1 109 688	1 098 310±300	11 378±300	12 353	975±300
38	(1 287 811) <sup>b</sup>	(1 273 994) <sup>c</sup>	(13 817)	14 808	(991)
40	(1 493 118) <sup>b</sup>	(1 476 605) <sup>c</sup>	(16 513)	17 587	(1074)
41	1 607 004	(1 588 921) <sup>c</sup>	(18 083)	19 199	(1116)
42	(1 729 001) <sup>b</sup>	1 709 431±585	19 570±585	20 711	1141±585
44	(1 999 182) <sup>b</sup>	(1 976 212) <sup>c</sup>	(22 970)	24 211	(1241)
45	(2 148 373) <sup>b</sup>	(2 123 533) <sup>c</sup>	(24 840)	26 123	(1283)
47	(2 477 592) <sup>b</sup>	(2 448 739) <sup>c</sup>	(28 853)	30 220	(1367)
50	(3 057 097) <sup>b</sup>	(3 021 360) <sup>c</sup>	(35 736)	37 228	(1492)

<sup>a</sup>Reference 7, Table II less finite nuclear size effects.

<sup>b</sup>Our interpolations from Tables III and IV, Ref. 3.

<sup>c</sup>Interpolation from experimental data.

effects. The next column gives the one-electron Lamb shift, as calculated by Johnson and Soff,<sup>7</sup> with finite-nuclear-size corrections subtracted, as these are included<sup>3</sup> in the  $\sigma_c$ . Similar data for the  $s_{1/2}-p_{3/2}$  transition are presented in Table III.

The differences between the observed  $\Delta(c-x)$  and the one-electron Lamb shifts are presumably due to the screening of the Coulomb field of the nucleus by the 1s electrons. These differences are given in the last columns of Tables II and III and are shown graphically in Fig. 1 for the  $s_{1/2}-p_{1/2}$  transition, and Fig. 2 for  $s_{1/2}-p_{3/2}$ .

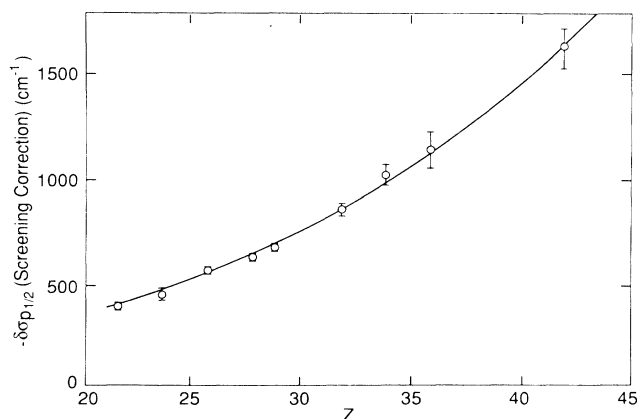


FIG. 1. Difference between the discrepancy of calculated and measured wave numbers  $\Delta(c-x)$  and the calculated one-electron QED effects vs  $Z$  for the  $s_{1/2}-p_{1/2}$  transitions. The solid curve is Eq. (2).

The curve drawn in Fig. 1 is the weighted least-squares fit to the data points. It has the equation

$$-\delta\sigma = 583.9 - 45.02Z + 1.666Z^2. \quad (2)$$

The uncertainties in the wave-number differences diverge rather rapidly in Fig. 2, because of the short wavelengths of these lines. However, the straight line

$$-\delta\sigma = -598.0 + 41.81Z \quad (3)$$

shown in the figure gives a reasonable fit to the data points.

Equations (2) and (3) may be extended slightly to higher  $Z$  values with reasonable accuracy. We have

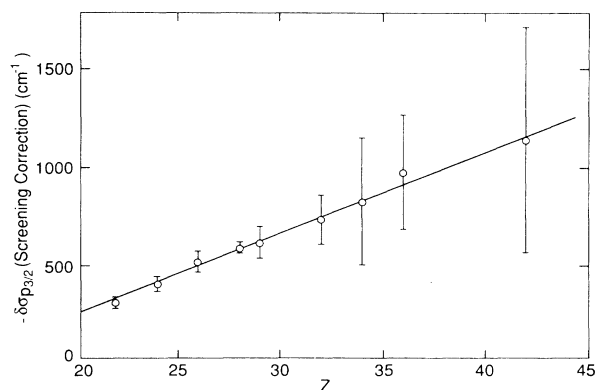


FIG. 2. As in Fig. 1 for the  $s_{1/2}-p_{3/2}$  transitions. The straight line is Eq. (3).

TABLE IV. Predicted wavelengths (in Å) for the lithiumlike doublet according to Eqs. (2) and (3) and the data in Tables II and III.

$Z$	$s_{1/2}-p_{1/2}$	$s_{1/2}-p_{3/2}$
38	162.983	78.493
40	153.027	67.723
41	148.425	62.936
44	135.764	50.602
45	131.915	47.091
47	124.686	40.837
50	114.890	33.098

therefore extended the interpolation of Tables II and III to  $Z = 50$ , for the benefit of future experiments. The corresponding wavelengths are given in Table IV.

We should also like to compare our present results with the extrapolated semiempirical values of Edlén.<sup>8</sup> As was noted in an earlier publication<sup>9</sup> based on poorer experimental data, there is evidence of a systematic deviation, in the sense of Edlén's wavelengths being increasing-

ly too short at higher  $Z$ . Nevertheless, his formulas are remarkably successful—even at molybdenum ( $Z = 42$ ) they predict wavelengths within 0.05 Å of our measured values.

A calculation of the QED contributions to the  $s_{1/2}-p_{1/2}$  and  $s_{1/2}-p_{3/2}$  transition energies has recently been published by Seely.<sup>10</sup> The transition energies derived by combining the QED contributions with the calculated energies of Ref. 3 are in excellent agreement with our experimental energies throughout the range of  $Z$  investigated in the present work. Excellent agreement is also obtained with the recent semiempirical predictions by Curtis.<sup>11</sup>

#### ACKNOWLEDGMENTS

We would like to thank Alan Ramsey and Brent Stratton at TFTR and George Magyar at JET for a variety of valuable contributions to this paper. The close cooperation between the authors was made possible by several visits under the Large Tokamak Tripartite Agreement. This work was partly supported by the U.S. Department of Energy, under Contract No. DE-AC02-76-CHO-3073.

<sup>1</sup>B. Denne, G. Magyar, and J. Jacquinet, *Phys. Rev. A* (to be published).

<sup>2</sup>H. G. Berry, R. DeSerio, and A. E. Livingston, *Phys. Rev. A* **22**, 998 (1980).

<sup>3</sup>W. R. Johnson, S. A. Blundell, and J. Sapirstein, *Phys. Rev. A* **37**, 2764 (1988).

<sup>4</sup>B. Denne, E. Hinnov, J. Ramette, and B. Saoutic, *Phys. Rev. A* **40**, 1488 (1989).

<sup>5</sup>B. Edlén and B. Löfstrand, *J. Phys. B* **3**, 1380 (1970).

<sup>6</sup>J. D. Garcia and J. E. Mack, *J. Opt. Soc. Am.* **55**, 654 (1965).

<sup>7</sup>W. R. Johnson and G. Soff, *At. Data Nucl. Data Tables* **33**, 405 (1985).

<sup>8</sup>B. Edlén, *Phys. Scr.* **28**, 51 (1983).

<sup>9</sup>B. Denne and E. Hinnov, *Phys. Scr.* **35**, 811 (1987).

<sup>10</sup>J. F. Seely, *Phys. Rev. A* **39**, 3682 (1989).

<sup>11</sup>L. J. Curtis, *Phys. Scr.* **39**, 447 (1989).